Acta Crystallographica Section D
Biological Crystallography
ISSN 0907-4449

The anticancer agent ellipticine unwinds DNA by intercalative binding in an orientation parallel to base pairs

Albert Canals,[a]* Mònica Purciolas,[a] Joan Aymamí[a,b] and Miquel Coll[a]

[a]Institut de Biologia Molecular de Barcelona, Consejo Superior de Investigaciones Científicas, Parc Científic de Barcelona, Baldiri Reixac 10-12, 08028 Barcelona, Spain, and [b]Departament d'Enginyeria Química, Universitat Politècnica de Catalunya, Diagonal 647, 08028 Barcelona, Spain

Correspondence e-mail: acpcri@ibmb.csic.es

Received 15 March 2005
Accepted 13 May 2005

PDB Reference: ellipticine–DNA complex, 1z3f, r1z3fsf.

Ellipticine is a natural plant product that has been found to be a powerful anticancer drug. Although still unclear, its mechanism of action is considered to be mainly based on DNA intercalation and/or the inhibition of topoisomerase II. Many experimental data suggest an intercalation based on stacking interactions along the major base-pair axis, but alternative binding modes have been proposed, in particular for ellipticine derivatives. The 1.5 Å resolution structure of ellipticine complexed to a 6 bp oligonucleotide unveils its mode of binding and enables a detailed analysis of the distorting effects of the drug on the DNA.

1. Introduction

Ellipticine (5,11-dimethyl-6*H*-pyrido[4,3-b]carbazole; Fig. 1) is a natural plant alkaloid originally isolated from *Ochrosia elliptica* of the *Apocynaceae* family that has been found to be a potent antitumour agent (for a review, see Garbett & Graves, 2004). Many of its more soluble derivatives, which have different DNA-binding affinities, show antitumour and cytotoxic effects and exhibit promising results in the treatment of breast-cancer metastases, kidney sarcomas, brain tumours and myeloblastic leukaemia (Stiborová *et al.*, 2001). Although a multimodal mechanism of action on DNA is accepted (Auclair, 1987), the effects of ellipticine derivatives are considered to mainly be based on DNA intercalation and/or the inhibition of topoisomerase II. Unfortunately, the exact mechanism remains unclear as a faithful binding mode has not been fully depicted to date. An early X-ray crystallographic structure of ellipticine complexed with a self-complementary ribodinucleoside monophosphate (Jain *et al.*, 1979; NDB code DRBB11) shows that the drug binds as a parallel base-stacking intercalator, similar to cryptolepine (Lisgarten *et al.*, 2002), actinomycin (Shinomiya *et al.*, 1995) and acridine-type drugs (Adams *et al.*, 1999), which intercalate parallel to the base-pair hydrogen bonds and stack its aromatic rings into the DNA bases. This type of binding would be in keeping with the hydrodynamic studies that assigned to ellipticine an unwinding angle equivalent to that of the parallel base-stacking intercalator ethidium bromide (Kohn *et al.*, 1975), accepted as being approximately 26° (Wang, 1974). However, because of the short length of the oligonucleotide used by Jain and coworkers, it has been questioned whether that structure represents the real DNA-binding mode (Garbett & Graves, 2004). Also, molecular-dynamics simulations suggested an alternative binding mode for one of its most studied derivatives, 9-hydroxyellipticine (Elcock *et al.*, 1996). According to these, 9-hydroxyellipticine would

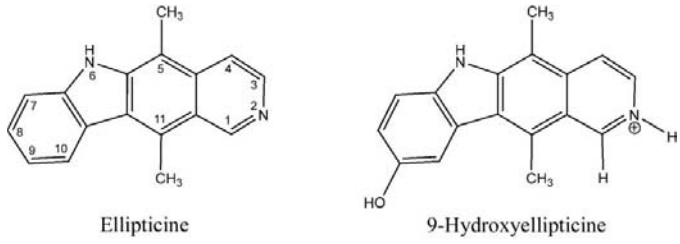

Figure 1
Chemical structure of ellipticine and the 9-hydroxyellipticine derivative.

intercalate in an orientation perpendicular to the long base-pair axis. As every derivative may have a different binding mode, extensive and accurate information on how the drugs of this family interact with DNA is needed in order to understand their mechanism of action. Here, we report the crystal structure determination of ellipticine in complex with a 6 bp DNA at 1.5 Å resolution, compare it with the previous crystallographic study of the same drug within a 2 bp structure and discuss the effect of ellipticine intercalation on DNA unwinding and lengthening.

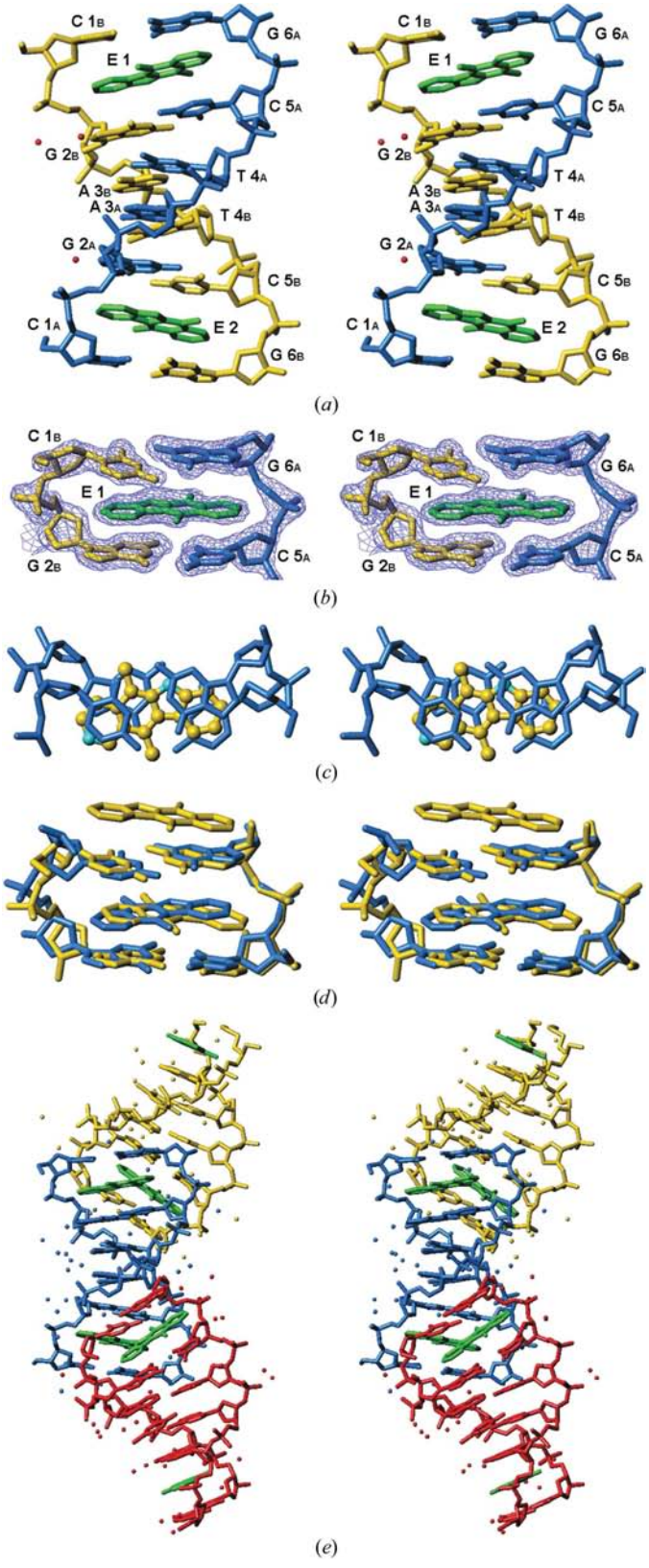

2. Materials and methods

2.1. Crystallization and data collection

Crystallization conditions were screened using the Nucleic Acid Mini Screen (Berger *et al.*, 1996). Yellow hexagonal crystals were grown at 293 K by the hanging-drop vapour-diffusion technique by mixing 2.0 µl 5 m*M* ellipticine, 1.0 µl 1.5 m*M* d(CGATCG)$_2$ and 1.0 µl crystallization solution (12% MPD, 40 m*M* sodium cacodylate pH 5.5, 20 m*M* cobalt hexammine, 12 m*M* sodium chloride and 80 m*M* potassium chloride) equilibrated against 500 µl 78% MPD. Both low- and high-resolution data sets were collected on a 130 mm MAR CCD detector (MAR Research) from a single crystal kept at 120 K using synchrotron radiation (λ = 0.976 Å) at the ESRF (Grenoble) microfocus beamline ID13. Data were indexed, integrated and scaled with the *XDS* package (Kabsch, 1993), yielding an $R_{\rm merge}$ of 8.7% and a completeness of 99.6% in the resolution range 16.7–1.5 Å. Data-collection statistics are shown in Table 1.

2.2. Structure solution and refinement

The structure was solved by molecular replacement with *AMoRe* (Navaza, 1994) using the DNA coordinates of the d(CGTACG)–D232 structure (Shui *et al.*, 2000; NDB code DD0018) as a starting model. Reflections within the resolution range 16.7–3.0 Å were used for rotation- and translation-function calculations. One clear solution was found with a correlation coefficient of 54.8% and a crystallographic *R* factor of 46.8% (values for the second highest peak are 46.0 and 49.6%, respectively). Refinement followed with *REFMAC*5 (Murshudov *et al.*, 1999). The optimum orientation of the intercalated ellipticine was identified by placing the drug in each of the four possible positions and refining until the best fit and corresponding best *R* factor and $R_{\rm free}$ were found. At this stage, an iterative refinement procedure was carried out using *REFMAC*5 with *ARP*/*wARP* (Perrakis *et al.*, 1999), interspersed with inspection of electron-density maps, water positioning and manual model rebuilding with *TURBO-FRODO* (Roussel & Cambillau, 1989). All data were used (16.7–1.5 Å) with no low-resolution or σ cutoff. A randomly selected 221 reflections (5%) were set aside for $R_{\rm free}$ calculations. The final refinement statistics are shown in Table 1. The helical parameters of the DNA were analyzed with the program *CURVES* (Lavery & Sklenar, 1988).

Figure 2
Stereoviews of the ellipticine–DNA complex. (*a*) The bis-intercalated d(CGATCG)$_2$ hexanucleotide forming an asymmetric unit. The drug and each strand of the DNA are represented in different colours. Red spheres represent Co atoms. (*b*) $2F_{\rm o} - F_{\rm c}$ electron-density map at the area of the intercalated ligand, looking into the minor groove. The map was contoured at the 1.0σ level. (*c*) Projection down the helix axis of a d(CpG)-d(GpC) dinucleotide with the sandwiched ligand. (*d*) Superimposition of the structure from Jain *et al.* (1979) in yellow and the equivalent part of the present structure in blue. (*e*) Three asymmetric units illustrating the crystal packing of the ellipticine–d(CGATCG)$_2$ structure. The drug is always coloured green and symmetry neighbours are in a different colour. Water molecules (spheres) are included.

Table 1
Data- and structure-quality statistics for the ellipticine–d(CGATCG)$_2$ complex at 1.5 Å resolution.

Values in parentheses are for the outer resolution shell (1.50–1.54 Å).

Data quality	
Resolution (Å)	16.7–1.5
R_{merge} (%)	8.7 (32.8)
Mean $I/\sigma(I)$	9.3 (4.6)
Completeness (%)	99.6 (99.7)
Multiplicity	5.2 (4.5)
Refinement	
Data/parameter ratio	3.6
No. nucleic acid atoms	240
No. drug atoms	38
No. metal atoms	3 (Co)
No. solvent waters	27
Resolution used in refinement (Å)	16.7–1.5
R_{cryst}	0.22 (0.24)
R_{free}	0.24 (0.35)
R.m.s. deviation, bonds (Å)	0.012
R.m.s. deviation, angles (°)	2.505
B values (Å^2)	
$C1_A$–$G6_B$	31.40–27.48
E2	27.59
$G2_A$–$C5_B$	30.02–32.67
$A3_A$–$T4_B$	27.03–28.58
$T4_A$–$A3_B$	27.99–26.77
$C5_A$–$G2_B$	32.10–30.39
E1	29.22
$G6_A$–$C1_B$	30.12–31.48
Average B value	30.95

3. Results and discussion

The ellipticine–d(CGATCG)$_2$ complex crystallizes in the hexagonal space group $P6_5$, with unit-cell parameters a = 24.86, b = 24.86, c = 78.86 Å. The asymmetric unit consists of a DNA duplex plus two drug molecules. The self-complementary hexamer adopts the double-helical B-DNA conformation with an ellipticine molecule intercalated between the CpG steps at both ends of the duplex (Fig. 2*a*). All atoms for both DNA and drug molecules have been modelled in and are well defined, as indicated by the quality of the electron-density maps (Fig. 2*b*). Inspection of $2F_o - F_c$ density maps contoured at the 4.0σ level revealed three putative hexammine cobalt molecules. The exact location of their amine moieties could not be determined and only the metal atom was added to the final model.

As might be expected owing to its shape and planar structure, ellipticine intercalates by stacking interactions with DNA base pairs (Fig. 2*c*). By these stacking interactions, ellipticine is aligned with its major axis parallel to the Watson–Crick hydrogen bonds of the base pairs. Despite sharing a common shape with cryptolepine, the different distribution of N atoms and methyl residues in ellipticine leads to a slightly different intercalation (Lisgarten *et al.*, 2002). Nitrogen N2 of both drug molecules faces the major groove of the DNA. None of the drug molecules are hydrogen-bonded to the DNA. Whereas one ellipticine molecule (E1) is kept in the intercalation site solely by stacking interactions, nitrogen N2 of the other molecule (E2) participates in a hydrogen bond with a water molecule (15W). The structure confirms that ellipticine has a strong preference for the d(GpC)-d(CpG) site, as no drug molecules are sandwiched in the d(ApT)-d(TpA) site. The three hydrogen bonds between G and C bases guarantee a tighter and thus more favourable site for intercalating a planar structure such as ellipticine.

In essence, the intercalation mode is similar to that described by Jain *et al.* (1979) in the structure of the complex of ellipticine with a self-complementary ribodinucleoside monophosphate. When superimposing the X-ray structures (Fig. 2*d*), the r.m.s. deviation for the positions of common C1′ atoms is 0.87 Å. They have similar sugar–phosphate backbone geometry, with a mixed sugar-puckering pattern C3′-*endo*/C2′-*endo* at the immediate site of drug intercalation. There is only a minor deviation of the ellipticine molecule position.

The ellipticine–d(CGATCG)$_2$ complex is tightly packed in the crystal, allowing only a 23% solvent content (27 water molecules in the final asymmetric unit). A peculiar end-to-side interaction between asymmetric units is the basis of the crystal packing. The C1–G6 base pair of one end of the complex invades the major groove of a neighbouring complex at the A3pT4 step and is held there by a direct hydrogen bond between the N1 of guanine G6 and O4′ of adenine A3 and two water-mediated hydrogen bonds (O6 of guanine G6 and O1 of phosphate from thymine T4, through water 18 W; O3′ of cytosine C5 and O1 of phosphate from guanine 6A, through water 3W). This pattern of interactions is repeated in a reciprocal way, so that every complex is both invaded and an invader at each end, as shown in Fig. 2(*e*). Water molecules mediate the other packing interactions between complexes.

As a result of the intercalation, the DNA is unwound and lengthened (Fig. 3). The DNA in the complex has a B-like conformation with Watson–Crick base pairing. However, in accommodating the intercalated ellipticine molecule, the DNA assumes conformational parameters that are significantly different from average B-DNA values. The DNA helical twist at the $C1_ApG2_A$-$G6_BpC5_B$ and $C5_ApG6_A$-$G2_BpC1_B$ intercalation sites is 21.4 and 21.9°, respectively. This is an unwinding angle of approximately 14° with respect to standard B-DNA at the intercalation steps. The adjacent CpT steps show an almost canonical B-DNA conformation (overwinding: 3.2 and 0.6°), whereas the central ApT step is slightly unwound (6.8°). At

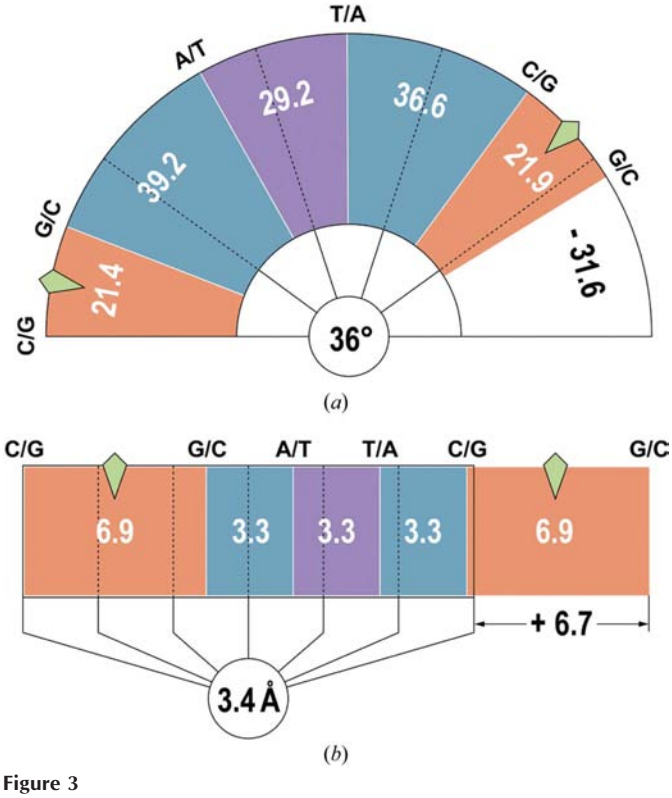

Figure 3
(*a*) Unwinding angle and (*b*) lengthening of the DNA in our crystals after ellipticine (green diamond) intercalation, according to the analysis made with the program *CURVES* (Lavery & Sklenar, 1988). Black lines indicate the expected inter-base-pair rotation angles and distances for an average drug-free B-DNA with the same sequence generated with *TURBO-FRODO* (Roussel & Cambillau, 1989). Coloured blocks with white values depict the actual winding and length between contiguous base-pairs in our structure. Overall differences are given in black.

both intercalation sites, the bases are separated by 6.9 Å. To achieve this major opening of the bases, the sugar–phospate backbone is distorted as discussed earlier.

Although the structure of ellipticine in complex with DNA strongly suggests a similar binding for its derivatives, other binding modes for the members of the ellipticine family cannot be ruled out. They may be as diverse as their cytotoxic or anticancer effects. Further structural studies should confirm if the binding mode described here also applies for the whole drug family.

This work was supported by the Ministerio de Educación y Ciencia de España (grants BIO2002-03964 and GEN2003-20642-CO9-01) and by the Generalitat de Catalunya (grant SGR2001-00346). Synchrotron data collection was supported by the European Synchrotron Radiation Facility (ESRF) and the EU.

References

Adams, A., Guss, J. M., Collyer, C. A., Denny, W. A. & Wakelin, L. P. G. (1999). *Biochemistry*, **38**, 9221–9233.
Auclair, C. (1987). *Arch. Biochem. Biophys.* **259**, 1–14.
Berger, I., Kang, C., Sinha, N., Wolters, M. & Rich, A. (1996). *Acta Cryst.* D**52**, 465–468.
Elcock, A. H., Rodger, A. & Richards, W. G. (1996). *Biopolymers*, **39**, 309–326.
Garbett, N. C. & Graves, D. E. (2004). *Curr. Med. Chem. Anti-Canc. Agents*, **4**, 149–172.
Jain, S. C., Bhandary, K. K. & Sobell, H. M. (1979). *J. Mol. Biol.* **135**, 813–840.
Kabsch, W. (1993). *J. Appl. Cryst.* **26**, 795–800.
Kohn, K. W., Waring, M. J., Glaubiger, D. & Friedman, C. A. (1975). *Cancer Res.* **35**, 71–76.
Lavery, R. & Sklenar, H. (1988). *J. Biomol. Struct. Dyn.* **6**, 63–91.
Lisgarten, J. N., Coll, M., Portugal, J., Wright, C. W. & Aymamí, J. (2002). *Nature Struct. Biol.* **9**, 57–60.
Murshudov, G. N., Lebedev, A., Vagin, A. A., Wilson, K. S. & Dodson, E. J. (1999). *Acta Cryst.* D**55**, 247–255.
Navaza, J. (1994). *Acta Cryst.* A**50**, 157–163.
Perrakis, A., Morris, R. & Lamzin, V. S. (1999). *Nature Struct. Biol.* **6**, 458–463.
Roussel, A. & Cambilleau, C. (1989). *Silicon Graphics Partners Directory*, pp. 77–79. Mountain View, CA, USA: Silicon Graphics.
Shinomiya, M., Chu, W., Carlson, R. G., Weaver, R. F. & Takusagawa, F. (1995). *Biochemistry*, **34**, 8481–8491.
Shui, X., Peek, M. E., Lipscomb, L. A., Wilkinson, A. P., Williams, L. D., Gao, M., Ogata, C., Roques, B. P. & Garbay-Jaureguiberry, C. (2000). *Curr. Med. Chem.* **7**, 59-71.
Stiborová, M., Bieler, C. A., Wiessler, M. & Frei, E. (2001). *Biochem. Pharmacol.* **62**, 1675–1648.
Wang, J. C. (1974). *J. Mol. Biol.* **89**, 783–801.